THE JOURNAL OF BIOLOGICAL CHEMISTRY VOL. 288, NO. 16, pp. 11287–11293, April 19, 2013
© 2013 by The American Society for Biochemistry and Molecular Biology, Inc. Published in the U.S.A.

Allosteric Transitions Direct Protein Tagging by PafA, the Prokaryotic Ubiquitin-like Protein (Pup) Ligase*[S]

Received for publication, November 12, 2012, and in revised form, February 14, 2013 Published, JBC Papers in Press, March 7, 2013, DOI 10.1074/jbc.M112.435842

Naomi Ofer[‡], Nadav Forer[‡], Maayan Korman[‡], Marina Vishkautzan[§], Isam Khalaila[¶], and Eyal Gur[‡§1]

From the [‡]Department of Life Sciences, the [§]National Institute for Biotechnology in the Negev, and the [¶]Avram and Stella Goldstein-Goren Department of Biotechnology Engineering, Ben-Gurion University of the Negev, Beer-Sheva 84105, Israel

Background: The interaction of PafA, the prokaryotic ubiquitin-like ligase, with its protein substrates is poorly understood.
Results: Measurements of PafA kinetics reveal cooperative substrate binding and experiments with engineered substrates suggest that PafA forms dimers.
Conclusion: The PafA enzymatic mechanism involves allosteric transitions.
Significance: PafA interaction with its target substrates is regulated at the enzyme level.

Protein degradation via prokaryotic ubiquitin-like protein (Pup) tagging is conserved in bacteria belonging to the phyla Actinobacteria and Nitrospira. The physiological role of this novel proteolytic pathway is not yet clear, although in *Mycobacterium tuberculosis*, the world's most threatening bacterial pathogen, Pup tagging is important for virulence. PafA, the Pup ligase, couples ATP hydrolysis with Pup conjugation to lysine side chains of protein substrates. PafA is the sole Pup ligase in *M. tuberculosis* and apparently, in other bacteria. Thus, whereas PafA is a key player in the Pup tagging (*i.e.* pupylation) system, control of its activity and interactions with target protein substrates remain poorly understood. In this study, we examined the mechanism of protein pupylation by PafA in *Mycobacterium smegmatis*, a model mycobacterial organism. We report that PafA is an allosteric enzyme that binds its target substrates cooperatively and find that PafA allostery is controlled by the binding of target protein substrates, yet is unaffected by Pup binding. Analysis of PafA pupylation using engineered substrates differing in the number of pupylation sites points to PafA acting as a dimer. These findings suggest that protein pupylation can be regulated at the level of PafA allostery.

Protein degradation via ubiquitin tagging was long thought to be a uniquely eukaryotic proteolytic pathway. In the last few years, however, it has become clear that bacterial species belonging to the phyla Nitrospira and Actinobacteria possess a tagging and degradation pathway that is highly analogous to the eukaryotic ubiquitin-proteasome pathway (1). Initially discovered in *Mycobacterium tuberculosis*, the bacterial ubiquitin-like tagging pathway conjugates Pup[2] to lysine side chains of protein substrates, thereby targeting them for proteasomal degradation (2). *M. tuberculosis*, like other actinobacterial species, contains a proteasome in addition to other smaller proteases, such as ClpXP and FtsH (3–5). Because Pup is recognized by Mpa, the proteasomal regulatory subunit, tagged (*i.e.* pupylated) proteins are degraded (6–10). Puppylation-deficient *M. tuberculosis* mutants are viable, but their virulence is compromised. Specifically, such mutants are sensitized to reactive nitrogen intermediates, antimicrobial compounds that are released into phagosomes by macrophages (11, 12). Noteworthy, the vast majority of Pup/proteasome-containing bacteria are nonpathogenic, suggesting a fundamental role of this proteolytic pathway in these species (13, 14).

Despite apparent functional similarity between Pup and ubiquitin, these degradation tags are not homologous. Unlike ubiquitin, Pup is a small, natively unstructured protein of 64 amino acids (7 kDa) that presents a GGE motif at its C terminus (2, 15, 16). Conjugation of Pup to protein substrates occurs through formation of an isopeptide bond between the γ-carboxylate of the C-terminal glutamate of Pup and an ϵ-amine group of a substrate lysine (2, 17). Like ubiquitin, Pup is activated by ATP hydrolysis prior to its conjugation (18, 19). However, the enzymatic mechanism of Pup activation and conjugation is altogether different from that of ubiquitin (1, 20). The Pup ligase, an enzyme termed PafA (proteasomal accessory factor A), both activates and conjugates Pup to protein substrates in a two-step reaction that is typical of glutamine synthetases and γ-glutamyl cysteine synthetases (2, 14, 19). Indeed, PafA was identified as a distant homologue of this group of enzymes (14). The first step in the PafA-catalyzed reaction is the phosphorylation of Pup on the γ-carboxylate of its C-terminal glutamate. Next, PafA catalyzes a nucleophilic attack on the phosphorylated carboxylate by the ϵ-amine group of a substrate lysine (19). For pupylation and PafA binding, only the C-terminal region of Pup is required, and whereas the N-terminal region of the protein is required for interaction with Mpa, it is expandable for pupylation (8, 9). In *M. tuberculosis* and many other related species, Pup is translated with a glutamine, rather than a glutamate at its C terminus. In these bacteria, a PafA-homologous enzyme termed Dop (deamidase of Pup) converts

* This work was supported in part by the German-Israeli Foundation Grant I-2230-2055.13/2009.
[S] This article contains supplemental Figs. S1 and S2 and supplemental Experimental Procedures.
[1] To whom correspondence should be addressed: Life Sciences Department and the National Institute of Biotechnology in the Negev, Ben-Gurion University, Rager Blvd., Beer-Sheva 84105, Israel. Tel.: 972-3-6472930; Fax: 972-3-6479114; E-mail: gure@bgu.ac.il.
[2] The abbreviations used are: Pup, prokaryotic ubiquitin-like protein; Ni^{2+}-NTA, nickel-nitrilotriacetic acid; Pup^{E}, deamidated Pup; TEV, tobacco etch virus.

this glutamine to a glutamate, thereby rendering Pup available for PafA conjugation (21).

Despite remarkable progress in understanding the pupylation system, it remains poorly understood how PafA interacts with its protein substrates and how such interactions are regulated. PafA is the only Pup ligase identified to date; and in *M. tuberculosis*, no pupylation is detected in *pafA* mutants (2). Understanding the enzymatic mechanism by which PafA interacts with its substrates is central to the understanding of this novel proteolytic pathway. Furthermore, PafA is important for *M. tuberculosis* virulence, and, as such, detailed mechanistic analysis of this enzyme may prove useful in the global combat against this pathogen.

In this study, we analyzed protein pupylation by PafA from *Mycobacterium smegmatis*. *M. smegmatis* is a commonly used mycobacterial model bacterium, with a PafA that is 94% identical to that of *M. tuberculosis*. We find that PafA is an allosteric enzyme that binds its target substrates cooperatively. In contrast, binding of deamidated Pup (Pup^E) by PafA follows simple kinetics and is, therefore, not involved in the allosteric transitions of PafA. We also find that Pup and target substrate binding by PafA are independent events. Analysis of engineered chimeric substrates that differ in the number of pupylation sites suggested that PafA is active as a dimer. In view of these findings, we propose that protein pupylation can be regulated at the enzyme level via an allosteric mechanism.

EXPERIMENTAL PROCEDURES

Protein Purification—All proteins, except a nontagged PanB, carried N-terminal polyhistidine tags and were expressed from plasmid pSH21 under the transcriptional control of the T7 promoter. Expression was at 37 °C, unless stated otherwise, in *Escherichia coli* ER2566 (New England Biolabs). Cells were lysed by sonication, and purification using Ni^{2+}-NTA-agarose (Qiagen) was carried out according to a standard protocol. For PafA and PanB, purification Ni^{2+}-NTA buffers contained 10% glycerol (v/v). As a consequent purification step, proteins were loaded onto a Superdex 75 size exclusion column (GE Healthcare) equilibrated with 25 mM Tris-HCl, pH 8.0 (hereafter, T25) for the titin-I27 variants, with pupylation buffer (50 mM Tris-HCl, pH 7.5, 100 mM KCl, 20 mM $MgCl_2$, and 10% (v/v) glycerol) for PafA and with T25, 50 mM NaCl, and 10% glycerol for polyhistidine-tagged PanB.

For Pup^E purification, *pup*^{E} was cloned into plasmid pSH21 in fusion with DNA encoding titin-I27 and a TEV protease recognition sequence (His_6-I27-TEV-Pup^E). Expression was at 30 °C, and Ni^{2+}-NTA purification was carried out as above. Following TEV cleavage, a buffer exchange step was carried out, and the His_6-I27-TEV portion of the chimera was removed by loading the solution onto a Ni^{2+}-NTA column. The flow-through was collected, and Pup^E was further purified on a C18 reverse phase column, lyophilized, and resuspended in T25.

For purification of Fl-Pup^E, a variant encoding a N-terminal cysteine was cloned (*i.e. his*$_6$*6 i27-tev-cys-pup*^{E}). Labeling with 5-iodoacetamidofluorescein was carried out following binding of the protein to the Ni^{2+}-NTA column. After excess 5-iodoacetamidofluorescein was washed, purification proceeded as for Pup^E.

To purify a PanB variant that does not carry a polyhistidine tag, *panB* was cloned into plasmid pET11a, and the protein was expressed at 37 °C in *E. coli* ER2566. The cell pellet was suspended in T25 containing 10% glycerol (v/v), and the cells were disrupted by sonication. Following centrifugation (12,000 × *g*, 15 min), streptomycin sulfate (1% (w/v)) was added to the clear lysate for precipitation of nucleic acids; and, following centrifugation as above, the supernatant was loaded onto an anionic exchange column (HiPrep Q FF; GE Healthcare) pre-equilibrated with T25 containing 10% glycerol (v/v). A NaCl gradient (0–1 M) was used for elution. PanB-containing fractions were pooled, concentrated, and loaded onto a size exclusion column (Superdex 200; GE Healthcare) pre-equilibrated with T25, 50 mM NaCl, 10% glycerol (v/v). As a final purification step, a Mono Q column was used (GE Healthcare), and following a buffer exchange step into T25, 50 mM NaCl, 10% glycerol (v/v) using a PD10 column (GE Healthcare), protein aliquots were stored at −80 °C until use.

Assays—Pupylation assays were carried out at 30 °C by mixing PafA, Pup^E, and a target substrate in pupylation buffer. Reactions were initiated with the addition of ATP to a final concentration of 2 mM. Quantitative pupylation assays relied on the use of a polyhistidine-tagged target substrate and the use of Fl-Pup^E instead of Pup^E. Initial rates were measured by collecting 10-μl aliquots at intervals during the reactions into tubes containing 50 μl of T25 and 6 M guanidine HCl (hereafter, T25G). Next, samples were diluted such that each contained equal concentrations of a polyhistidine-tagged target protein. 50 μl of each diluted sample was transferred into filter microcentrifuge tubes (Corning ZQ-VW-8169) containing 50 μl of Ni^{2+}-NTA-agarose beads equilibrated with 500 μl of T25G. Following a 2-min incubation, the liquid was removed by centrifugation (7000 × *g*, 3 min), and beads were washed twice with 500 μl of T25G. Elution was carried out by resuspension of the beads in T25G, 250 mM imidazole, and centrifugation as above. The fluorescence intensity of each sample was measured with a Synergy 2 microplate reader (Biotek instruments) at 485 nm (excitation) and 528 nm (emission).

For Fl-Pup^E-PafA binding assays, the proteins were mixed in pupylation buffer without ATP or target substrates. Fluorescence anisotropy was measured as above.

LC/MS analysis, bioinformatics, and pupylation site identification are described in supplemental Experimental Procedures.

RESULTS

Cooperative Substrate Binding by PafA—To study the interaction of *M. smegmatis* PafA with protein substrates, pupylation of a *bona fide* target substrate was examined. Earlier studies indicated that *M. tuberculosis* PanB (ketopantoate hydroxymethyltransferase), a homodecameric protein complex, is pupylated efficiently by the *M. tuberculosis* PafA both *in vitro* and *in vivo* (2, 9, 22). To test *in vitro* pupylation by the *M. smegmatis* system, the *M. smegmatis panB*, *pafA*, and *pup*^{E} genes were cloned, and their encoded proteins were purified to homogeneity. In a reaction including ATP and Pup^E, the formation of a pupylation product with a molecular mass approximately 7 kDa heavier than PanB suggested that each PanB monomer was singly pupylated by PafA (Fig. 1*A*, *left*). MS/MS analysis indicated

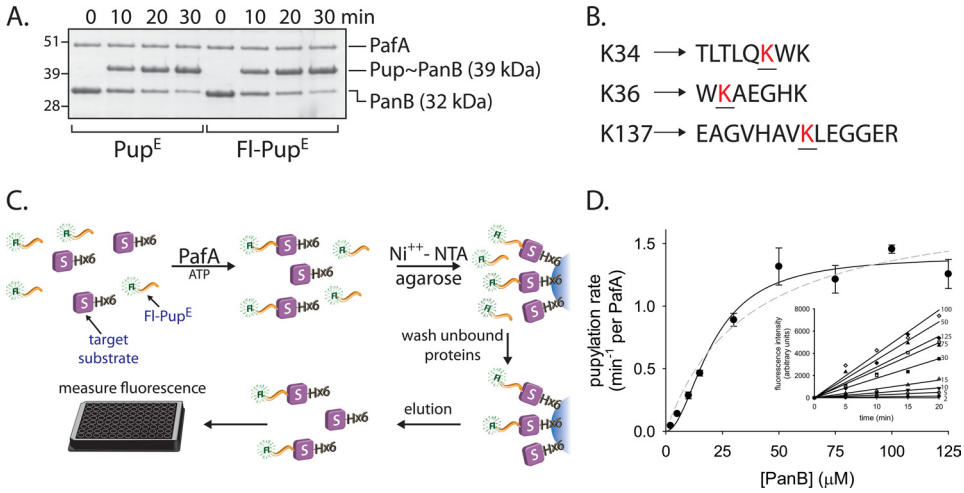

FIGURE 1. **PafA pupylation of PanB, a *bona fide* substrate.** *A*, SDS-PAGE analysis of PanB (5 μM) pupylation by PafA (1 μM) and Pup^E or Fl-Pup^E (10 μM each) is shown. Following electrophoresis, Coomassie Brilliant Blue was used for staining. *B*, PanB pupylation sites (*red*) in tryptic peptides that were identified by MS/MS analysis are denoted. *C*, the use of Fl-Pup^E and a polyhistidine-tagged target substrate allows removal of unconjugated Fl-Pup^E via Ni^{2+}-NTA chromatography. The fluorescence intensity of the eluate thus provides a quantitative measure of end product formation. *D*, steady-state rates of PafA (0.5 μM)- and Fl-Pup^E (15 μM)-mediated pupylation as a function of increasing polyhistidine-PanB concentration. The data were fitted to the Hill equation (rate $= V_{max}\cdot[S]^n/(K_{0.5}{}^n + [S]^n)$; *solid line*) and to the Henri-Michaelis-Menten equation (rate $= V_{max}\cdot[S]/(K_m + [S])$; *dashed line*). The averages ± S.D. (*error bars*) of three experiments are presented. Pupylation rates were derived from the measurements presented in the *inset*.

that PanB is pupylated primarily on either one of two lysines, namely Lys^{34} or Lys^{36}. Pupylation on Lys^{137} was also detected, although less frequently (Fig. 1*B* and supplemental Fig. S1). Next, a quantitative assay able to examine *M. smegmatis* PafA pupylation kinetics was sought. Although the pupylation kinetics of *M. tuberculosis* PafA have been previously examined by monitoring the first half of the pupylation reaction cycle (*i.e.* ATP hydrolysis and Pup^E phosphorylation) (19), we wanted to analyze the full PafA reaction cycle to gain further insight into the interaction of PafA with target substrates. To this end, a quantitative pupylation assay was developed using an N-terminally fluorescein-labeled Pup^E variant (Fl-Pup^E). As Pup^E and Fl-Pup^E were conjugated equally well to protein substrates by PafA (Fig. 1*A*), Fl-Pup^E was used for quantitative pupylation analysis instead of unlabeled Pup^E. This novel assay, described under "Experimental Procedures," allows quantitative measurements of end product formation by the use of Fl-Pup^E and a polyhistidine-tagged target substrate in a PafA-dependent reaction (Fig. 1*C*).

Titration experiments were carried out in which steady-state pupylation rates were measured at a constant Fl-Pup^E concentration and increasing PanB concentrations (Fig. 1*D*). The obtained data can be described by a sigmoidal rate equation (Fig. 1*D*), suggesting PanB binding by PafA to be cooperative. A Hill coefficient of 1.9 ± 0.3 (Table 1) indicates that PafA oligomers with at least two binding sites are involved in PanB pupylation. The kinetic measurements revealed a $K_{0.5}$ of 21 ± 2 μM for PanB pupylation and a V_{max} of 1.4 ± 0.1 Fl-Pup^E conjugations per min per PafA monomer (Table 1). As the assays were carried out in the presence of a saturating Fl-Pup^E concentration, the maximal pupylation rate is equivalent to the catalytic rate constant (k_{cat}) of the reaction. Both the $K_{0.5}$ and V_{max} measured for PanB pupylation closely matched the published values for *M. tuberculosis* PanB pupylation by *M. tuberculosis* PafA (19).

TABLE 1
Steady-state kinetic parameters for the PafA-catalyzed reactions measured in this work

Substrate	V_{max}	$K_{0.5}$	Hill coefficient
	min^{-1}*/PafA*	μM	
PanB	1.4 ± 0.1[a]	21 ± 2	1.9 ± 0.3
$I27_1$	1.4 ± 0.1[a]	534 ± 87	1.6 ± 0.2
$I27_2$	1.4 ± 0.1[a]	348 ± 42	1.3 ± 0.1
$I27_3$	1.3 ± 0.1[a]	368 ± 45	1.2 ± 0.08
Pup	0.14 ± 0.01	1.3 ± 0.4	0.94 ± 0.2

[a] The values are equivalent to the k_{cat} of the reactions, as measurements were carried out at saturating Pup^E concentrations.

Cooperative substrate binding, as depicted in Fig. 1*D*, suggests that PafA is an allosteric enzyme. A hallmark of enzyme allostery is the positive effect of a competitive inhibitor on substrate processing at low inhibitor and substrate concentrations (23). An increase in enzymatic activity detected under such conditions can be attributed to stabilization of an active or high affinity enzyme conformation by the inhibitor. As a result, certain low inhibitor concentrations can lead to both inhibition and activation, such that the net effect is a facilitated substrate-processing rate (23). Similar kinetics can also be observed using a competing substrate rather than a competitive inhibitor (24). To test whether such an allosteric behavior is present in our system, pupylation reactions were carried out at a fixed low concentration of polyhistidine-PanB and at increasing concentrations of a PanB variant lacking the polyhistidine tag. As detection of pupylation in the quantitative assays employed in this study relies on the use of polyhistidine-tagged substrates (Fig. 1*B*), nontagged PanB thus acts as a competitor. Nevertheless, at low competitor concentrations, increased pupylation of polyhistidine-PanB was observed, providing further evidence of PafA allostery (Fig. 2*A*). In the presence of higher concentrations of nontagged PanB, competition dominates, resulting in a decrease in pupylation of the polyhistidine-tagged substrate (Fig. 2*A*). To test whether binding of a target lysine is sufficient to induce an allosteric PafA transition, a similar experiment was carried out, this time titrating free lysine instead of nontagged

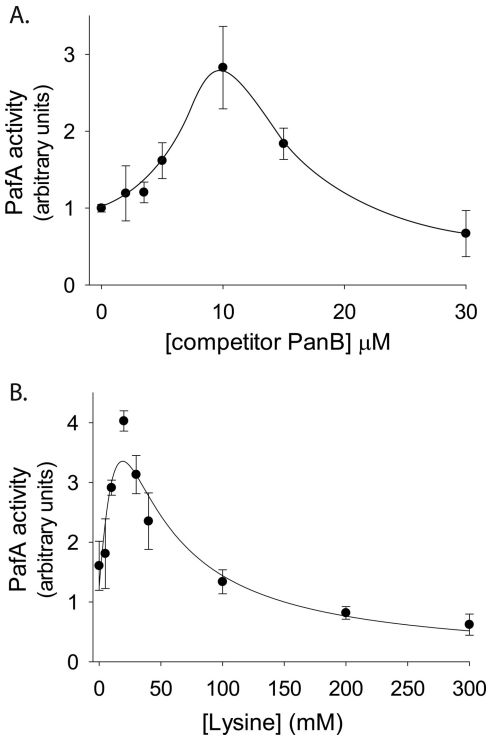

FIGURE 2. **Allosteric activation by a competitor substrate.** *A*, steady-state rates of a polyhistidine-PanB (1 μM) pupylation by PafA (0.5 μM) and Fl-Pup^E (15 μM) at increasing concentrations of nontagged competitor PanB. The values presented were obtained following subtraction of background fluorescence values measured in reactions lacking polyhistidine-PanB. The *solid curve* is a guide to the eye. *B*, as in *A*, but with free lysine (pH 8.0) instead of nontagged PanB competitor. The curve is fitted to the equation rate = $C{\cdot}\alpha{\cdot}(1+\alpha+\beta)/(L+(1+\alpha+\beta)^2)$, where C is a scaling factor, α = [polyhistidine-PanB]/K_m = 1/21, β = [Lys]/$K_{0.5}$, and L is a conformational equilibrium constant (27). In both *A* and *B*, the averages ± S.D. (*error bars*) of three experiments are presented.

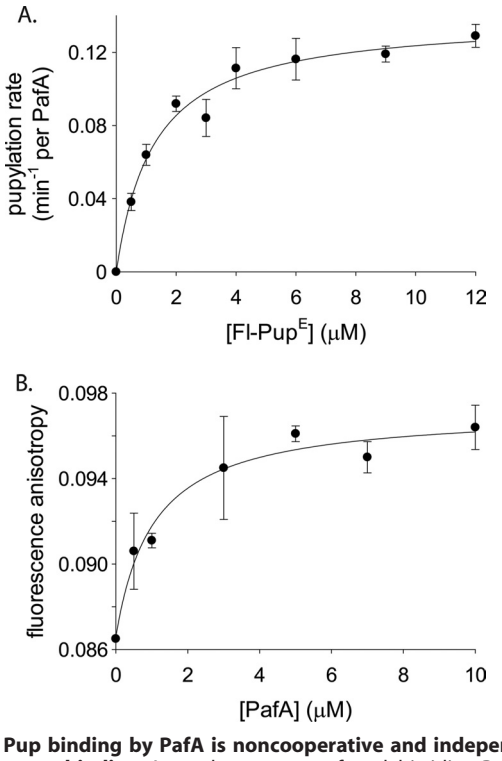

FIGURE 3. **Pup binding by PafA is noncooperative and independent of target substrate binding.** *A*, steady-state rates of a polyhistidine-PanB (1 μM) pupylation by PafA (0.25 μM) at increasing Fl-Pup^E concentrations. The curve is fitted to the Hill equation. *B*, fluorescence anisotropy of Fl-Pup^E (50 nM) at increasing PafA concentrations. The curve is fitted to the binding equation, $r = r_0 + (r_{max}{\cdot}[\text{PafA}])/(K_D + [\text{PafA}])$, where r is the fluorescence anisotropy value. In both *A* and *B*, the averages ± S.D. (*error bars*) of three experiments are presented.

PanB. Again, a clear allosteric effect was observed at low lysine concentrations, whereas at higher concentrations, pupylation of polyhistidine-PanB was inhibited (Fig. 2*B*). Noticeably, the lysine concentrations required for induction of an allosteric PafA transition were approximately 1000-fold higher than the PanB concentrations that induced a similar effect (Fig. 2*A*). These differences are consistent with the ~1000-fold lower affinity of PafA for free lysine (~22 mM) compared with its affinity for PanB (~21 μM) (Table 1 and Ref. 19).

Pup^E Is Not Involved in Allosteric PafA Transitions—The mode of Pup^E binding to PafA was next considered when pupylation of low polyhistidine-PanB concentrations was measured at increasing Fl-Pup^E concentrations. Data fitting to the Hill equation yielded a nonsigmoidal curve with a Hill coefficient of 0.94 ± 0.2, indicating that Pup^E is not cooperatively bound by PafA nor does Pup^E affect binding of the target protein substrate to PafA (Fig. 3*A* and Table 1). The $K_{0.5}$ value measured for Fl-Pup^E (1.3 ± 0.3 μM; Fig. 3*A* and Table 1) closely matched the K_D for Fl-Pup^E binding to PafA, as measured in a direct binding assay in the absence of a nucleophile substrate (0.86 ± 0.3 μM; Fig. 3*B*). Therefore, binding of Pup^E to PafA is not affected by the binding of the target substrate. These results thus indicate that binding of Pup^E and a target substrate to PafA are independent events. This conclusion is further supported by the similarity between the obtained affinity values and the apparent binding constant measured for the interaction of *M. tuberculosis* Pup^E with *M. tuberculosis* PafA in the absence of a target substrate (19).

A Dimer-based Model for PafA-Substrate Interaction—Cooperative substrate binding by PafA indicates that the active form of this enzyme is oligomeric. Indeed, *Corynebacterium glutamicum* PafA, an orthologue of the molecule considered here, was recently crystallized in the asymmetric unit as a dimer where swapping of an N-terminal β-strand and a concomitant α-helix was shown (25). Nonetheless, efforts to determine the stoichiometry of *M. smegmatis* PafA oligomers using classic methods, such as size exclusion chromatography and analytical ultracentrifugation, have been hampered by the low solubility of *M. smegmatis* PafA, as was also reported for *M. tuberculosis* PafA (19). As an alternative approach, we instead tested the pupylation of chimeric substrates presenting different numbers of pupylation sites. To this end, concatemeric variants of a non-native substrate protein, the I27 domain of human Titin, were used. Titin-I27 is a globular domain that can be easily unfolded *in vitro* by chemical modification (*e.g.* carboxymethylation) of its two cysteines (26). We found unfolded titin-I27 to be pupylated substantially faster than was the folded form of the protein (supplemental Fig. S2*A*). It was also noted that titin-I27 is pupylated primarily on a single lysine, as determined by SDS-PAGE and mass spectrometry (Fig. S2, *A* and *B*). To examine the impact on pupylation kinetics upon encountering multiple substrate pupylation sites, linear fusions of two and three titin-I27 domains were constructed. Single titin-I27 and the resulting

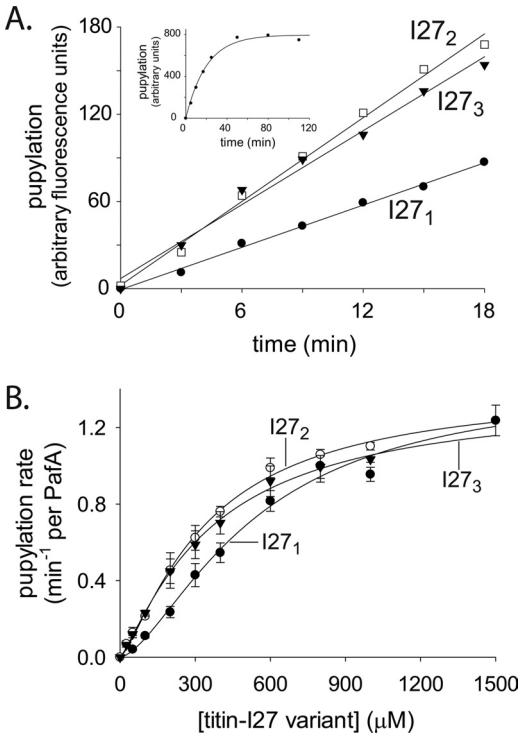

FIGURE 4. **PafA pupylation of titin-I27 variants.** *A*, pupylation of titin-I27 variants (15 μM each) by PafA (0.5 μM) and Fl-Pup^E (1 μM). The *inset* demonstrates an I27$_1$ pupylation reaction with PafA (0.5 μM) and Fl-Pup^E (7 μM) that continued to completion. *B*, steady-state pupylation rates by PafA (0.5 μM) and Fl-Pup^E (15 μM) at increasing concentrations of titin-I27 variants. The curves are fitted to the Hill equation. The averages ± S.D. (*error bars*) of three experiments are presented.

concatemeric proteins (denoted as I27$_1$, I27$_2$, and I27$_3$) were purified to homogeneity, unfolded by carboxymethylation, and the rates of their *in vitro* pupylation were compared (Fig. 4*A*). I27$_2$ was pupylated approximately twice as fast as was I27$_1$, as expected, given that I27$_2$ contains two pupylation sites, as opposed to the single such site in I27$_1$. However, no additional increase in rate was observed for pupylation of I27$_3$. Rather, this substrate was pupylated as fast as was I27$_2$ and again about twice as fast as was I27$_1$ (Fig. 4*A*). To better assess the pupylation kinetics of each titin-I27 variant, titration assays were carried out by measuring pupylation rates at different substrate concentrations (Fig. 4*B*). No significant differences in the value of V_{max} (~1.4 min^{-1} per PafA) were detected (Fig. 4*B* and Table 1). By contrast, the $K_{0.5}$ value for pupylation of I27$_1$ (534 ± 87 μM; Table 1) was found to be nearly 2-fold higher than that of I27$_2$ (348 ± 42 μM) or of I27$_3$ (368 ± 45 μM). These results suggest that the rate differences observed in Fig. 4*A* arise mainly from affinity effects. A Hill coefficient of 1.6 ± 0.2 for I27$_1$ pupylation suggested cooperative binding of this titin-I27 variant by PafA, as in the case of PanB pupylation (Table 1). Notably, PafA binding of the I27$_2$ and I27$_3$ concatemers occurred with a lower degree of cooperativity, as determined by Hill coefficients of 1.3 ± 0.1 and 1.2 ± 0.08, respectively (Table 1). We thus conclude that the pupylation kinetics of the titin-I27 variants are consistent with PafA being active as a dimer. As illustrated in Fig. 5*A*, binding of the first target lysine of I27$_2$ can lead to an increase in the local concentration of the second target lysine near a free PafA binding site. As a result, binding of the second I27$_2$ target lysine is highly favorable, with the flexibility of the unfolded titin-I27 domains enabling binding without steric constrains that might otherwise limit the binding of folded proteins. A dimer-based model also explains the higher degree of cooperativity observed for I27$_1$ pupylation. Indeed, binding of I27$_2$ or I27$_3$ to a PafA dimer cannot lead to stabilization of a free substrate binding site, thus preventing cooperative binding of an additional substrate. Finally, the existence of only two binding sites explains why elongation of I27$_2$ by an additional unit to generate I27$_3$ does not improve binding.

A dimer-based model, as illustrated in Fig. 5*A*, predicts I27$_1$ to be singly pupylated and I27$_2$ to be doubly pupylated. Importantly, according to this model, I27$_3$ should be only doubly pupylated despite presenting three pupylation sites. These predictions were indeed verified when pupylation of the titin-I27 variants was examined by SDS-PAGE (Fig. 5*B*). Noticeably, dual pupylation of I27$_2$ and of I27$_3$ proceeded without the formation of gel bands corresponding to single I27$_2$ and I27$_3$ pupylation intermediates. This suggests that following the initial pupylation of either I27$_2$ or I27$_3$, the second pupylation event occurs very fast and probably without substrate release. This further suggests that a third I27$_3$ pupylation event can occur, yet requires substrate release (following double pupylation) and rebinding. In agreement with this rationale, a third pupylation event was indeed observed for I27$_3$ when pupylation was allowed to proceed over an extended period of time (Fig. 5*C*).

DISCUSSION

By establishing a quantitative pupylation assay, we were able to measure the kinetics of *M. smegmatis* PafA pupylation in this study. Thus, using a *bona fide* PafA substrate, PanB, cooperative binding by PafA could be observed for the first time, suggesting that PafA is an allosteric enzyme. This conclusion was further supported by competition assays in which substrate pupylation was facilitated at low competitor concentrations. These experiments further indicated that binding of the target lysine to PafA is sufficient to induce the allosteric effect.

There are a number of ways in which binding of a target substrate to PafA can facilitate the pupylation rate. For example, binding of a target lysine by PafA can enhance its affinity to Pup^E, thereby facilitating pupylation at undersaturating Pup^E concentrations. Such a model, however, is highly unlikely, as our data clearly indicate that binding of Pup^E and the binding of target substrates by PafA are independent events. Therefore, Pup^E does not play a role in the allosteric transitions that are reflected in the experiments presented here. Rather, the data can be explained by the existence of alternative PafA conformations that differ either in their affinity for target substrates or in their catalytic activity. This scenario requires that the binding of target substrates to PafA would stabilize the high affinity or the more active conformation.

A Hill coefficient of 1.9 ± 0.3 for PanB pupylation (Table 1) indicates that the minimal oligomeric form of PafA is dimeric. Cooperative substrate binding was also evident when pupylation of titin-I27 was examined. In addition, these assays indicated that elongation of I27$_1$ by an additional titin-I27 unit resulted in an approximately 2-fold increase in affinity, as reflected in the $K_{0.5}$ values measured for the titin-I27 variants.

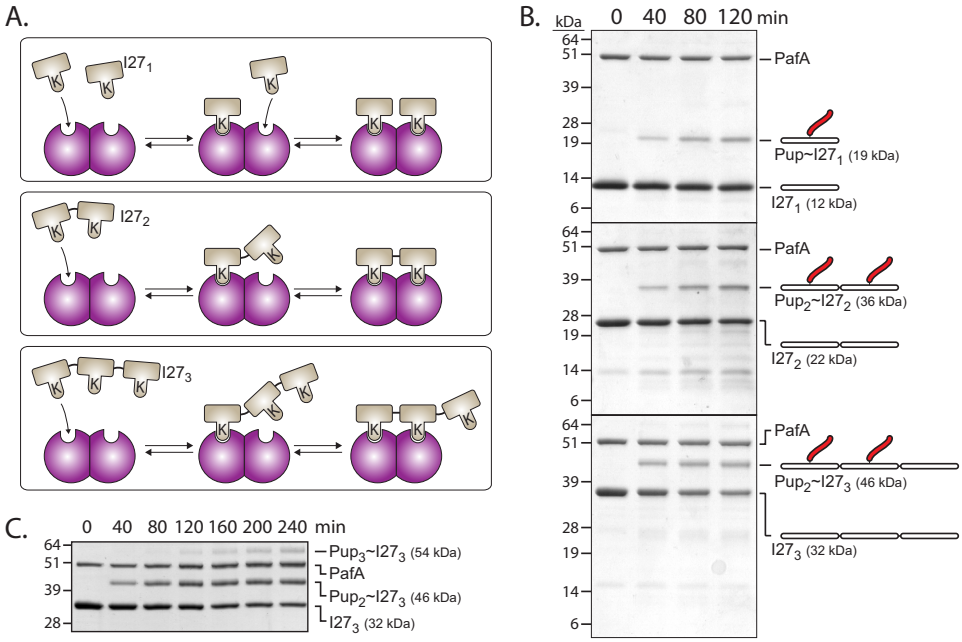

FIGURE 5. **A two-binding site model for PafA interaction with titin-I27 concatemers.** *A*, two adjacent PafA subunits (*purple*) can bind two $I27_1$ monomers, one $I27_2$ monomer, or two target lysines in $I27_3$. *B*, SDS-PAGE analysis of pupylation by PafA (1.0 μM) and Pup^E (25 μM) of $I27_1$ (12 μM), $I27_2$ (6 μM), and $I27_3$ (4 μM). Following electrophoresis, Coomassie Brilliant Blue was used for staining. *C*, pupylation of $I27_3$ as in *C* is shown, but for a longer reaction time.

However, elongation by yet another titin-I27 unit to generate $I27_3$ did not improve affinity to PafA. These results are in perfect correlation with the number of Pup molecules that were conjugated to each titin-I27 variant. In other words, the 2-fold increase in the affinity of $I27_2$ and $I27_3$, compared with $I27_1$, was accompanied by an additional Pup molecule attached to these chimeric substrates. These observations can be explained by the existence of PafA oligomers containing two binding sites, as illustrated in Fig. 5*A*. A dimer-based model is also consistent with the reduced cooperativity observed for $I27_2$ and $I27_3$, compared with $I27_1$. Our results suggest that following binding of the first target lysine of $I27_2$ or $I27_3$, binding of the second lysine occurs almost simultaneously. This would explain the absence of detectable singly pupylated $I27_2$ and $I27_3$ in our steady-state kinetics assays. An almost simultaneous accommodation of both binding sites of a PafA dimer by $I27_2$ or $I27_3$ would result in a 2-fold increase in the pupylation rate. This interaction would, however, prevent facilitated binding of the next substrate molecule. Therefore, a less cooperative binding of $I27_2$ and $I27_3$ is observed. Unlike $I27_2$ and $I27_3$, PanB is cooperatively bound by PafA. Thus, despite being a decamer, PanB does not simultaneously accommodate the two binding sites of a PafA dimer. This is likely because for decameric PanB to bind two PafA binding sites, the PanB target lysines must be positioned in a conformation that may not exist in the folded, rigid conformation of the decamer. $I27_2$ and $I27_3$, on the other hand, are unfolded and flexible, and can thus easily assume the conformation required for the simultaneous occupation of the two PafA binding sites.

A dimer-based model for PafA allostery is consistent with the recently published *C. glutamicum* PafA structure (25). Altogether, our kinetic data strongly suggest that the dimeric form is the correct biological assembly and the allosterically active conformation of the protein. We cannot exclude the possibility of dimeric PafA existing as part of a higher oligomeric form, such as a dimer of dimers or a trimer of dimers. Hence, additional studies are required to decipher the oligomeric state of biologically active PafA.

As the only Pup ligase currently known, PafA plays a most central role in deciding which proteins will be pupylated. It is, therefore, reasonable that the expression level and activity of PafA be tightly regulated *in vivo*. This study suggests that substrate pupylation *in vivo* can be regulated at the level of PafA allostery. For example, pupylation can be regulated by altering the equilibrium between an active oligomeric form and an inactive conformation. Further study will be required to understand the mechanistic details of PafA allostery and the role it plays in bacterial physiology.

Acknowledgments—We thank Bob Sauer (Massachusetts Institute of Technology), Boaz Shaanan, Amir Aharoni, and Ofer Yifrach (Ben-Gurion University) for helpful advice and fruitful discussions.

REFERENCES

1. Burns, K. E., and Darwin, K. H. (2010) Pupylation versus ubiquitylation: tagging for proteasome-dependent degradation. *Cell Microbiol.* **12,** 424–431
2. Pearce, M. J., Mintseris, J., Ferreyra, J., Gygi, S. P., and Darwin, K. H. (2008) Ubiquitin-like protein involved in the proteasome pathway of *Mycobacterium tuberculosis*. *Science* **322,** 1104–1107
3. Nagy, I., Tamura, T., Vanderleyden, J., Baumeister, W., and De Mot, R. (1998) The 20S proteasome of *Streptomyces coelicolor*. *J. Bacteriol.* **180,** 5448–5453
4. Knipfer, N., Seth, A., Roudiak, S. G., and Shrader, T. E. (1999) Species variation in ATP-dependent protein degradation: protease profiles differ between mycobacteria and protease functions differ between *Mycobacterium smegmatis* and *Escherichia coli*. *Gene* **231,** 95–104
5. Darwin, K. H., Lin, G., Chen, Z., Li, H., and Nathan, C. F. (2005) Characterization of a *Mycobacterium tuberculosis* proteasomal ATPase homologue. *Mol. Microbiol.* **55,** 561–571

6. Sutter, M., Striebel, F., Damberger, F. F., Allain, F. H., and Weber-Ban, E. (2009) A distinct structural region of the prokaryotic ubiquitin-like protein (Pup) is recognized by the N-terminal domain of the proteasomal ATPase Mpa. *FEBS Lett.* **583,** 3151–3157
7. Burns, K. E., Liu, W. T., Boshoff, H. I., Dorrestein, P. C., and Barry, C. E., 3rd (2009) Proteasomal protein degradation in *Mycobacteria* is dependent upon a prokaryotic ubiquitin-like protein. *J. Biol. Chem.* **284,** 3069–3075
8. Burns, K. E., Pearce, M. J., and Darwin, K. H. (2010) Prokaryotic ubiquitin-like protein provides a two-part degron to *Mycobacterium* proteasome substrates. *J. Bacteriol.* **192,** 2933–2935
9. Striebel, F., Hunkeler, M., Summer, H., and Weber-Ban, E. (2010) The mycobacterial Mpa-proteasome unfolds and degrades pupylated substrates by engaging Pup's N terminus. *EMBO J.* **29,** 1262–1271
10. Wang, T., Darwin, K. H., and Li, H. (2010) Binding-induced folding of prokaryotic ubiquitin-like protein on the *Mycobacterium* proteasomal ATPase targets substrates for degradation. *Nat. Struct. Mol. Biol.* **17,** 1352–1357
11. Darwin, K. H., Ehrt, S., Gutierrez-Ramos J. C., Weich, N., and Nathan, C. F. (2003) The proteasome of *Mycobacterium tuberculosis* is required for resistance to nitric oxide. *Science* **302,** 1963–1966
12. Cerda-Maira, F. A., Pearce, M. J., Fuortes, M., Bishai, W. R., Hubbard, S. R., and Darwin, K. H. (2010) Molecular analysis of the prokaryotic ubiquitin-like protein (Pup) conjugation pathway in *Mycobacterium tuberculosis*. *Mol. Microbiol.* **77,** 1123–1135
13. Lupas, A., Zwickl, P., and Baumeister, W. (1994) Proteasome sequences in eubacteria. *Trends Biochem. Sci.* **19,** 533–534
14. Iyer, L. M., Burroughs, A. M., and Aravind, L. (2008) Unraveling the biochemistry and provenance of pupylation: a prokaryotic analog of ubiquitination. *Biol. Direct* **3,** 45
15. Liao, S., Shang, Q., Zhang, X., Zhang, J., Xu, C., and Tu, X. (2009) Pup, a prokaryotic ubiquitin-like protein, is an intrinsically disordered protein. *Biochem. J.* **422,** 207–215
16. Chen, X., Solomon, W. C., Kang, Y., Cerda-Maira, F., Darwin, K. H., and Walters, K. J. (2009) Prokaryotic ubiquitin-like protein pup is intrinsically disordered. *J. Mol. Biol.* **392,** 208–217
17. Sutter, M., Damberger, F. F., Imkamp, F., Allain, F. H., and Weber-Ban, E. (2010) Prokaryotic ubiquitin-like protein (Pup) is coupled to substrates via the side chain of its C-terminal glutamate. *J. Am. Chem. Soc.* **132,** 5610–5612
18. Imkamp, F., Rosenberger, T., Striebel, F., Keller, P. M., Amstutz, B., Sander, P., and Weber-Ban, E. (2010) Deletion of dop in *Mycobacterium smegmatis* abolishes pupylation of protein substrates *in vivo*. *Mol. Microbiol.* **75,** 744–754
19. Guth, E., Thommen, M., and Weber-Ban, E. (2011) Mycobacterial ubiquitin-like protein ligase PafA follows a two-step reaction pathway with a phosphorylated pup intermediate. *J. Biol. Chem.* **286,** 4412–4419
20. Maupin-Furlow, J. (2012) Proteasomes and protein conjugation across domains of life. *Nat. Rev. Microbiol.* **10,** 100–111
21. Striebel, F., Imkamp, F., Sutter, M., Steiner, M., Mamedov, A., and Weber-Ban E. (2009) Bacterial ubiquitin-like modifier Pup is deamidated and conjugated to substrates by distinct but homologous enzymes. *Nat. Struct. Mol. Biol.* **16,** 647–651
22. Chaudhuri, B. N., Sawaya, M. R., Kim, C. Y., Waldo, G. S., Park, M. S., Terwilliger, T. C., and Yeates, T. O. (2003) The crystal structure of the first enzyme in the pantothenate biosynthetic pathway, ketopantoate hydroxymethyltransferase, from *M. tuberculosis*. *Structure* **11,** 753–764
23. Monod, J., Wyman, J., and Changeux, J. P. (1965) On the nature of allosteric transitions: a plausible model. *J. Mol. Biol.* **12,** 88–118
24. Gur E., and Sauer R. T. (2009) Degrons in protein substrates program the speed and operating efficiency of the AAA^+ Lon proteolytic machine. *Proc. Natl. Acad. Sci. U.S.A.* **106,** 18503–18508
25. Özcelik, D., Barandun, J., Schmitz, N., Sutter, M., Guth, E., Damberger, F. F., Allain, F. H., Ban, N., and Weber-Ban, E. (2012) Structures of Pup ligase PafA and depupylase Dop from the prokaryotic ubiquitin-like modification pathway. *Nat. Commun.* **3,** 1014
26. Kenniston, J. A., Baker, T. A., Fernandez, J. M., and Sauer, R. T. (2003) Linkage between ATP consumption and mechanical unfolding during the protein processing reactions of an AAA^+ degradation machine. *Cell* **114,** 511–520
27. Segel, IH (1975) *Enzyme Kinetics: Behavior and Analysis of Rapid Equilibrium and Steady-State Enzyme Systems*, pp. 421–461, John Wiley & Sons, New York